

Improved uncertainty evaluation for a long distance measurement by means of a temperature sensor network

Gertjan Kok¹, Federica Gugole¹, Aaron Seymour¹, Richard Koops¹

¹ VSL B.V., Thijssseweg 11, 2629 JA Delft, the Netherlands

ABSTRACT

The aim of the research described in this paper was to more accurately determine the measurement uncertainty of an interferometric long distance measurement. The chosen method was to install a temperature sensor network in the laboratory to measure in more detail the ambient temperature profile to more accurately determine the local values of the refractive index on the path travelled by the laser light. The experimental measurements were supplemented by a theoretical analysis of the mathematical model being used. The outcome of the performed work was that the claimed measurement uncertainty of the distance measurement, which is based on using only 5 temperature sensors, was justified. However, if in the future a lower uncertainty would be needed, a sensor network like the one that was temporarily installed would be needed. During the measurement campaign an offset in the mean temperature of 0.2 °C was found, which was equal to the maximum allowed bias in view of the claimed uncertainty for the long distance measurement. At a more general level, it was concluded that such sensor networks provide a useful new tool to increase the understanding of other measurements, to validate assumptions and optimize existing measurements.

Section: RESEARCH PAPER

Keywords: Sensor network; uncertainty; interferometry; temperature; refractive index

Citation: Gertjan Kok, Federica Gugole, Aaron Seymour, Richard Koops, Improved uncertainty evaluation for a long distance measurement by means of a temperature sensor network, Acta IMEKO, vol. 12, no. 1, article 14, March 2023, identifier: IMEKO-ACTA-12 (2023)-01-14

Section Editor: Daniel Hutzschenreuter, PTB, Germany

Received November 19, 2022; **In final form** February 14, 2023; **Published** March 2023

Copyright: This is an open-access article distributed under the terms of the Creative Commons Attribution 3.0 License, which permits unrestricted use, distribution, and reproduction in any medium, provided the original author and source are credited.

Funding: This project (17IND12 Met4FoF) has received funding from the EMPIR programme co-financed by the Participating States and from the European Union's Horizon 2020 research and innovation programme.

Corresponding author: Gertjan Kok, e-mail: gkok@vsl.nl

1. INTRODUCTION

One of the many aspects of the digital transformation is that sensor networks come at an affordable cost, are relatively easy to set up, and can measure with good accuracy once properly calibrated. As such they can be helpful to support other measurements by giving a greater understanding of the set-up, validate assumptions and improve uncertainty calculations. Examples of sensor networks supplementing high-grade measurements are sensor networks for measuring outdoor air quality [1] and for noise measurements [2]. Sensor networks are also advantageously being used in agriculture [3] and in aerospace applications [4].

This paper deals with a long-distance interferometric measurement, which will be supported by means of a sensor network for measuring ambient temperature. Various measurement schemes exist for interferometric distance measurements [5] and some of them have been implemented at

VSL [6], the Dutch National Metrology Institute (NMI). In this paper we consider the classical fringe counting Michelson interferometer [5].

The research question addressed by this paper was to validate a particular assumption that is currently used in the uncertainty calculation for interferometric measurements over long distances. This assumption was that the inhomogeneity of the air temperature was small enough that the current approach of using 5 temperature sensors over a total distance of 50 meters is sufficient. This assumption and the meaning of 'sufficient' will be made quantitative in Section 2.

In order to be able to validate this assumption two activities were undertaken. The first activity was the extension of the mathematical model describing the measurement from considering only the mean temperature over a long-distance path to account for the temperature profile over a path. This naturally led to additional theoretical questions regarding the exact shape of the light path, which were addressed by performing simulations, see Section 2. Secondly, we installed a sensor

network with 51 calibrated temperature sensors in VSL's 50 meter long climatized corridor in which highly accurate long distance measurements are performed. The knowledge of the air temperature along a path is essential for this application due to its effect on the refractive index of air. With the help of the temperature sensor network the uncertainty evaluation of the long distance measurement was improved.

This work was performed in the EMPIR project "Metrology for the Factory of the Future" in a task dedicated to redundant measurements of ambient conditions [7]. In this project several aspects related to sensor networks were studied, like redundancy aspects [8] or the effect of synchronization errors [9], based on various case studies in industrial testbeds.

The outline of this paper is as follows. In Section 2 the problem will be formulated with more mathematical detail, followed by a detailed presentation of the sensor network in Section 3. In Section 4 the results of both the simulations and the measurements will be presented. In the last section the overall conclusions are summarized.

2. PROBLEM DESCRIPTION

2.1. Measurement problem and approximations

The distance measurement takes place in a climatized laboratory in which the temperature is kept between 19.5 °C and 20.5 °C. In the set up distances up to 50 m are being measured by means of a Michelson interferometer with a laser light source with a vacuum wavelength $\lambda_{\text{vac}} = 633 \text{ nm}$. A measurement is performed by moving an optical target (retroreflector) from the initial position to the final position. The optical target is mounted on a cart which moves smoothly in a straight line on a rail such that the electronics can count the number of fringes m (not necessarily an integer). To convert this number to a measured distance D , it needs to be divided by two and multiplied by the actual wavelength in air λ . This wavelength is derived from the vacuum wavelength by multiplication with the refractive index n . The refractive index is evaluated using Edlen's formula [10] at the laser wavelength λ_{vac} , the measured mean air pressure, the measured mean relative humidity and the measured mean air temperature T_0 . Finally, using these mean values the resulting estimate D_0 of the distance is calculated by

$$D_0 = \frac{m}{2} \lambda_{\text{vac}} n(T_0). \quad (1)$$

The claimed expanded uncertainty for D_0 with coverage factor $k = 2$ is 1 ppm relative. In absolute terms this amounts to 50 μm at a measured distance of 50 m. Equation (1) is based on the following assumptions:

1. It is assumed that the non-linearity of the function $n(T)$ is weak and that it is sufficient to evaluate $n(T)$ at the mean temperature value only.
2. Due to local temperature variations, the light will be refracted and not travel in a perfect straight line, but on a curved path, leading to an overestimate of the distance. It's assumed that this effect is small.
3. It is assumed that the mean temperature can be estimated sufficiently well by measuring spot temperatures at only 5 positions.

The validity of assumptions 1 and 2 have been analysed in a theoretical way and the results are presented in Section 3.1 and 3.2. The validity of assumption 3 was assessed by means of installing a dedicated temperature sensor network. This network

will be presented in more detail in the next section. If the assumptions 1 and 3 are not fulfilled, a more complex model of the form

$$D_1 = \frac{m}{2} \lambda_{\text{vac}} \frac{1}{L} \int_0^L n(T(x)) dx \quad (2)$$

will be needed in which the full variation of the refractive index over the travel path of the laser light is considered. Here L denotes the nominal distance and $T(x)$ the temperature at position x along a path. In optics, the integral quantity in equation (2) is called the optical path length. If assumption 2 is not verified, then the model would become even more complex as the measured distance would depend on a three-dimensional profile of the refractive index. In that case a map of the temperature in three-dimensional space would be required.

2.2. Target uncertainty

In generic terms, an additional uncertainty contribution is not considered significant if it contributes less than about 1/5 of the current combined uncertainty. This is because the new combined uncertainty including the additional uncertainty component will have essentially the same size as $\sqrt{1^2 + 0.2^2} \approx 1$. Having this in mind, we will now assess what the maximum measurement bias of the mean ambient temperature can be, without significantly affecting the combined uncertainty of the long distance measurement.

The claimed combined expanded uncertainty at 50 m is 50 μm ($k = 2$). In view of the discussion of the last paragraph, the expanded uncertainty or maximum bias in the measured mean temperature should not contribute more than 1/5 of 50 μm , which is 10 μm . Using Edlen's formula, it can be calculated that a change of 1 °C in temperature induces a change in the calculated refractive index of slightly lower than 1 ppm, which results in a change of the calculated distance of 48 μm at a total measured distance of 50 m by means of equation (1). This indicates that the expanded uncertainty of the mean temperature should not be more than

$$\frac{10}{48} \cdot 1 \text{ °C} = 0.21 \text{ °C}. \quad (3)$$

For a potential systematic bias in the measurement temperature we are using the same threshold of 0.21 °C. The goal of the sensor network is to assess if the measurement bias when determining the mean temperature using only 5 temperature sensors compared to the improved estimate when using 51 sensors lies below this threshold. If this is indeed the case, the usual procedure using only 5 temperature sensors can be retained without a need for increasing the claimed uncertainty to account for a larger than expected uncertainty in the measured mean temperature.

3. TEMPERATURE SENSOR NETWORK

3.1. Construction of the network

Fifty-one temperature sensors were assembled in house in order to get the lowest measurement uncertainty. The sensing part consisted of a 10 k Ω NTC thermistor placed in series with a resistance of 12 k Ω . The communicating part was formed by Texas Instruments CC2531 USB Zigbee modules, communicating wirelessly at a frequency of 2.4 GHz. The voltage over the thermistor was measured by an analogue voltage input

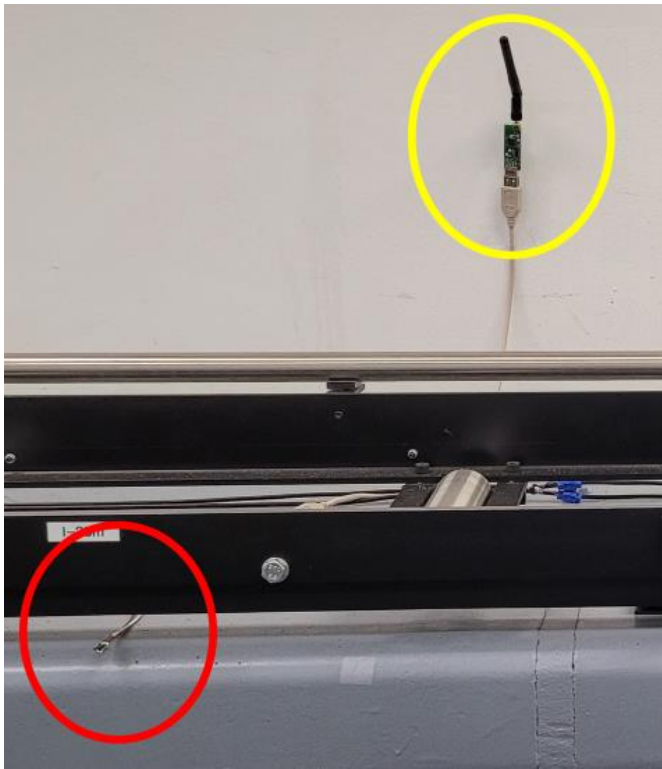


Figure 1. The horizontal black parts are the rails for the cart used in the interferometer set-up. In the red circle at the lower left corner the sensing part of a temperature sensor node is visible. In the yellow circle in the top right corner a router node with external antenna is visible, connected to the wire supplying power by means of a USB connector.

of the module. To enhance the stability of the network, 5 additional CC2531 chips with external antennae were used. Whereas the sensor nodes had only a meandered antenna on the chip itself, the external antennae more than tripled the link quality. The routers were used to repeat the network signal over the full distance of the measurement. To supply power to the nodes and routers a long wire with USB plugs at 1 meter spacing was used, as this seemed more practical than 51 individual battery packs. A Texas Instruments CC1352P chip was used as a coordinator in the network. Finally, a Raspberry Pi 3 Model A+ was used to run the Zigbee server to which voltage readings were also logged in real time. In Figure 1 a photo is shown with a temperature sensor mounted below the rail of the interferometric measurement cart set-up, together with a router node with external antenna. The total cost of the hardware was around 1000 EUR.

3.2. Calibration of the sensors

The sensors were calibrated in the following way. The sensors, together with a set of traceable reference sensors, were mounted on an aluminium block which could be brought to a desired temperature by means of a water-based heating and cooling device. The block and sensors were well isolated from the environment by means of an insulating box. The digital voltage output which was transmitted wirelessly, was calibrated and a calibration function relating voltage output to temperature was established. Calibration of all sensors took place before and after the measurement campaigns. After calibration, the expanded uncertainty of each of the sensors was $0.04\text{ }^{\circ}\text{C}$ ($k = 2$), mainly limited by the resolution of the digital voltage output of the sensors. This uncertainty includes a component for the repeatability over two days, but doesn't include a component for

the expected drift of the sensors over the entire measurement period.

3.3. Software

To operate the Zigbee network by means of the Raspberry Pi two pieces of software were used. The Zigbee2MQTT software [11] was used to start the Zigbee server. The Zigbee Mosquitto software [12] provides a messaging protocol which was used to interface with the coordinator. These two pieces of software ultimately allow for the text message transmissions containing the voltage readings from the ADCs of each of the sensor nodes to be stored on the Raspberry Pi. Appropriate firmware was installed at the sensor nodes [13] and at the coordinator node [14].

3.4. Test procedure

The main aim of the measurement campaign was to gain insight into the overall temperature profile along the corridor, and specifically, to assess if the mean value of the 5 climate system sensors was sufficiently close to the mean temperature of the 51 sensor network sensors, having the numerical target required for the interferometric distance measurement in mind as stated in equation (3). In order to get some further insights, a test plan with the following five test cases was defined:

1. Undisturbed profile with nobody present in the corridor
2. Person sitting at a fixed spot in the corridor
3. Person walking around in the corridor all the time
4. Person walking around in the corridor and then leaving the corridor
5. Profile during a long distance measurement with the moving cart

All sensors were calibrated in week 1. Then the test plan was executed in week 2 and repeated in week 3. In week 4 all sensors were recalibrated in order to assess their drift.

4. RESULTS

In this Section the results will be presented. They are ordered according to the assumptions to be verified as listed in Section 2.1.

4.1. Assumption 1 on non-linearity of refractive index formula

The effect of the neglected non-linearity of the refractive index as a function of temperature in equation (1) was analysed using a worst-case approach. If the mean temperature is $20.0\text{ }^{\circ}\text{C}$, then the worst case is that half of the path length is at $19.5\text{ }^{\circ}\text{C}$ and the other half at $20.5\text{ }^{\circ}\text{C}$. The effective average refractive index in this case then amounts to $(n(19.5\text{ }^{\circ}\text{C}) + n(20.5\text{ }^{\circ}\text{C}))/2$ which has to be compared with the value $n(20.0\text{ }^{\circ}\text{C})$ that is obtained from first averaging the temperature instead of averaging refractive indices, the latter begin what is currently used. The difference is only $6 \cdot 10^{-10}$ both in absolute and in relative sense, as $n \approx 1.0003$. The induced measurement error by averaging temperatures as done in equation (1) instead of averaging refractive indices therefore amounts to only $-6 \cdot 10^{-10} \times 50\text{ m} = -0.03\text{ }\mu\text{m}$ at a measurement distance of 50 m, which is very minor. The non-linearity of the refractive index dependence on temperature can therefore be neglected and for the uncertainty calculation of the interferometric long distance measurement it is sufficient to focus on the correct determination of the mean temperature.

4.2. Assumption 2 on curved light paths

If a light beam travels from one medium into another medium with a different refractive index (e.g., air with a different temperature), it will change its direction of propagation following Snell's law [15]:

$$n_1 \sin \theta_1 = n_2 \sin \theta_2, \quad (4)$$

where n_i and θ_i are respectively the refractive index and the angle of the propagation direction of the beam to the surface normal in medium $i = 1$ and 2. So the magnitude of the direction change $\theta_2 - \theta_1$ depends on the difference of the refractive indices and on the angle of incidence θ_1 .

Equation (1) is based on the assumption that the light travels in a perfectly straight line without any curvature due to diffraction. To assess how much this simplification affects the final measurement result D_0 two-dimensional curves were simulated by modelling the temperature distribution by a one-dimensional Gaussian process with a squared exponential kernel of the form

$$\sigma_T^2 \exp\left(-\frac{(x_1 - x_2)^2}{2 \ell^2}\right). \quad (5)$$

In equation (5), the parameters x_1 and x_2 denote the horizontal position of points 1 and 2 (horizontal distance from the laser emitting the light), ℓ the characteristic length-scale of the kernel, and σ_T the standard deviation of the temperature. This kernel defines the correlation strength between the temperatures at different positions in the corridor. The normal vectors of the interfaces between two neighbouring zones of uniform temperature were chosen randomly. In reality the situation is probably more favourable than this, as the interfaces will be more similar to planes perpendicular to the propagation direction of the light and not fully randomly oriented. In Figure 2, a schematic sketch of the simulated temperature profile together with the light path is shown. In our simulation we used 1000 zones of uniform temperature over a distance of 50 m. In this simulation only the geometric path length was assessed, thus the effect of different actual wavelengths due to changes in the refractive index in different path sections is not included in the results in this section. This latter effect is covered by the results of Sections 4.1 and 4.3. It was found that the maximum path increase significantly depended on the used parameter values. As a reasonable choice for the kernel parameters the characteristic

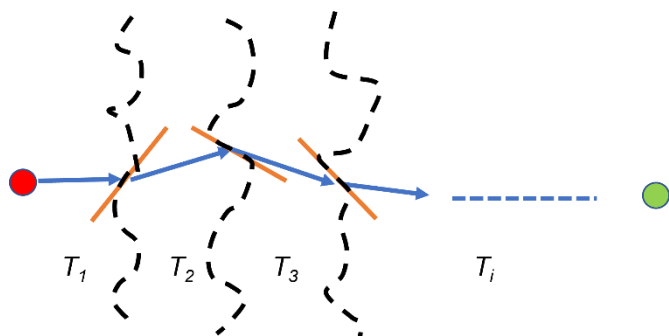


Figure 2. Two-dimensional simulation of curved light paths due to refraction effects. The vertical curvy black dashed lines delimit zones with different temperatures. The slanted orange lines indicate the assumed direction of the local interface between these zones. The light is assumed to travel from the red spot on the left to the green spot on the right and back.

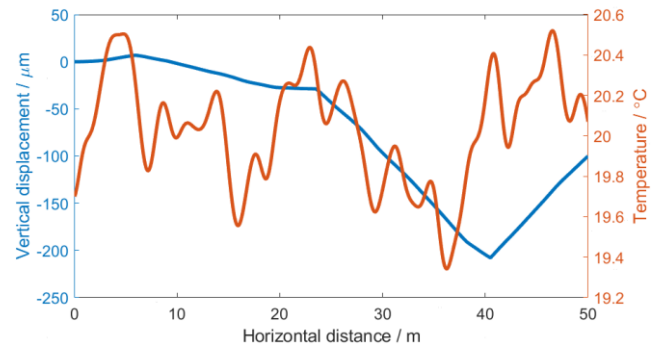


Figure 3. Blue: Simulated curved path of the light using 1000 zones of 50 mm width in which the temperature was assumed to be uniform. Red: Temperature profile over the distance of 50 m. Not shown are the angles defining the interfaces between the zones, which are completely random.

length-scale of correlation parameter was set to $\ell = 1$ m and the standard deviation of the temperature was set to $\sigma_T = 0.25$ °C, as the climate system kept the laboratory temperature between 19.50 °C and 20.50 °C. For this choice the simulated increase in path length remained below 1 μm , thus being negligible. In Figure 3, an example of a simulated path of the laser beam is shown.

Note nevertheless that one can mathematically construct worst-case temperature profiles with worst-case normal vectors in which the light travels an almost arbitrary path of arbitrary large distance, e.g., the light can change direction by 180°. For this to happen, the normal vectors should be chosen close to vertical and the temperature differences between zones should be chosen as large as possible.

4.3. Assumption 3 on the measured overall mean temperature

The test procedure with the temperature sensor network as specified in Section 3.4 was executed twice in two consecutive weeks. The main points of attention during the data analysis were the changes of the measurement values of the individual sensors over time, the spatial temperature profile of the mean sensor values in the corridor, and the comparison of the measured values by the 5 sensors of the fixed installed climate system and the 5 sensors of the sensor network that were in the closest proximity. After the first test campaign it turned out that some of the 51 sensors reported readings only sporadically, or not at all. Therefore fewer sensors were used during the second campaign. In the first campaign data from 40 sensors were available, whereas in the second campaign data from 30 sensors were used.

The temperature traces of single sensors over time were generally very stable, although incidentally some higher and/or lower values were measured. In Figure 4, the temperature profile in space for test case 5 simulating a real measurement is shown. As some measurement instruments and computers are present near the start of the corridor the temperature is slightly higher in that region. The temperature profiles for the other cases look similar.

We'll now first present the conclusions for the various test cases as defined in Section 3.4 before addressing our main question based on the uncertainty of the long distance measurement induced by the non-constant temperature profile.

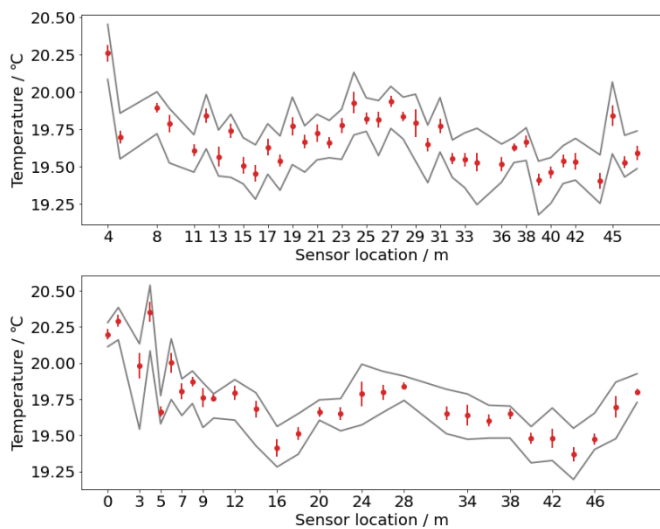


Figure 4. Temperature profile in space for test case 5 simulating a real measurement for the two repetitions A (top) and B (bottom). The circular marker is at the mean value and the error bars are at plus minus one standard deviation. The lines above and below connect the maximum and minimum measured values during the entire time span.

It turned out that the measurement results for the various test cases were not significantly different, as compared with the unperturbed case 1. In test case 2, a person sitting between two sensors did not cause any significant perturbation in the temperature measurements of the sensors. In test cases 3 and 4, a person walking around the lab caused significant perturbations in the sensors' reading during the first execution but not during the second. The results on this aspect were therefore inconclusive. During test case 5, a battery powered temperature sensor was mounted on the moving cart and its measured values were compared with the values of the non-moving sensors mounted closest by at the moment when the cart passed. The differences between the moving sensor network sensor and the non-moving sensor network sensors varied from 0.05 °C to a few 0.1 °C with a maximum of even 0.6 °C, which is higher than expected.

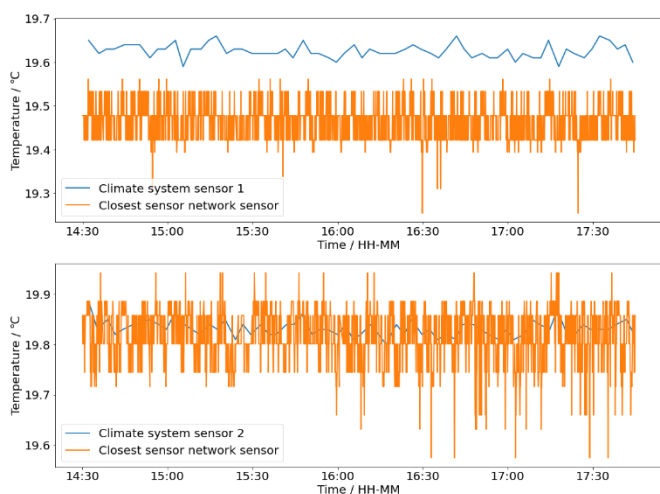


Figure 5. Measured temperature profile over time for two sensors of the climate system and the sensors of the sensor network that was installed at the closest position for test case 5-A. For the climate system sensor displayed in the upper plot there is a difference of about 0.15 °C, whereas for the measurement at the bottom there is complete agreement.

Furthermore, the values of the 5 fixed installed climate system sensors were compared with the values of the nearest sensors of the sensor network, both placed on the 50 meter long granite support for the interferometric measurement set-up. Two of the five climate sensors agreed well with the closest sensor network sensors within the mutual uncertainties, whereas a third sensor agreed part of the time. Two sensors didn't agree and differences of 0.15 to 0.20 °C were present between the mean values of the climate system sensors and the sensor network sensors. The differences can be due to the sensor hanging in free air or not, or to locally warmer air flows (one such a flow was detected close to an electrical device mounted half way the corridor). This indicates that the location of the sensors can be an important factor when measuring the temperature of the lab. In Figure 5, the temperature plots over time of two climate sensors together with the plots of the nearest sensor network sensors are shown.

We'll now turn to the results for the main purpose of our measurement campaigns, which was to determine if the mean temperature of the corridor was measured sufficiently well, with a bias below 0.21 °C. In Table 1, the mean temperatures as measured by the climate system and as measured by the sensor network including the uncertainties and their differences are shown. The uncertainty of both the climate system and the sensor network was dominated by a systematic part due to the calibration, supplemented by a part for the variation during the measurement. Based on the recalibration of the sensor network sensors after the measurement campaigns a standard uncertainty for sensor drift of 0.05 °C was added per sensor. However, as it was a random contribution, it averaged out when calculating the mean temperature and it didn't affect the uncertainty of the mean value.

As can be seen from Table 1, it turned out that the difference between the mean corridor temperature as measured by the sensor network and the climate system was at most 0.25 °C with an expanded uncertainty of 0.06 °C. When using the expanded measurement uncertainty as a tolerance, the threshold of 0.21 °C of equation (3) was not exceeded. It was therefore decided that it is not needed to improve the temperature measurement in the corridor for this application in a permanent way, nor to increase the claimed uncertainty. However, the results also indicated that if the claimed uncertainty were to be reduced in future, then a better understanding of the temperature profile would be needed. This could then be accomplished by the sensor network, albeit that its potential drift over time would need a more careful study.

Table 1. Mean temperature and expanded uncertainty ($k = 2$) in parentheses as measured by the climate system and by the sensor network, and their differences, as measured in the 5 test cases and the two test campaigns A and B.

Case number	Climate System / °C	Sensor network / °C	Difference / °C
1-A	19.91 (0.06)	19.67 (0.03)	0.24 (0.06)
1-B	19.89 (0.06)	19.73 (0.03)	0.16 (0.06)
2-A	19.92 (0.06)	19.69 (0.03)	0.24 (0.06)
2-B	19.93 (0.06)	19.75 (0.03)	0.18 (0.06)
3-A	19.94 (0.06)	19.70 (0.03)	0.25 (0.06)
3-B	19.91 (0.06)	19.76 (0.03)	0.15 (0.06)
4-A	19.91 (0.06)	19.68 (0.03)	0.23 (0.06)
4-B	19.90 (0.06)	19.75 (0.03)	0.15 (0.06)
5-A	19.93 (0.06)	19.73 (0.02)	0.20 (0.06)
5-B	19.92 (0.06)	19.76 (0.03)	0.16 (0.06)

5. CONCLUSIONS

The digital transformation makes it economically and practically possible to perform a larger number of measurements in a much finer spatial grid by means of sensor networks. This can help to better monitor the ambient measurement conditions of a measurement set-up and as a consequence potentially reduce its measurement uncertainty. In this contribution a sensor network with 51 sensors for measuring the ambient temperature in a corridor used for interferometric long distance measurements was presented. This network enabled the analysis of the temperature profile in much more detail than what was possible until recently, together with a more accurate measurement of the mean temperature. Simulation results showed that it is sufficient to focus on the mean temperature only, as well as that the effect of a non-straight optical path due to refraction effects is negligible. The measurement results using the network showed that the mean temperature measured by the 5 climate system sensors was on average about 0.2 °C higher than the more accurate measurement by the sensor network. Based on this result it was decided that the current practice with only five temperature measurements and a claimed relative measurement uncertainty of 1 ppm is valid. In future work the network can be used in other applications where temperature measurement is of critical importance. Furthermore, employment and recalibration at longer time scales will give more information about the metrological stability of such sensor networks.

ACKNOWLEDGEMENTS

This project (17IND12 Met4FoF) has received funding from the EMPIR programme co-financed by the Participating States and from the European Union's Horizon 2020 research and innovation programme.

We thank the independent reviewers for their comments, which helped to significantly improve the paper.

REFERENCES

- [1] D. R. Peters, O. A. M. Popoola, R. L. Jones, N. A. Martin, J. Mills, E. R. Fonseca, A. Stidworthy, E. Forsyth, D. Carruthers, M. Dupuy-Todd, F. Douglas, K. Moore, R. U. Shah, L. E. Padilla, R. A. Alvarez, Evaluating uncertainty in sensor networks for urban air pollution insights, *Atmos. Meas. Tech.*, 15, 2022, pp. 321–334. DOI: [10.5194/amt-15-321-2022](https://doi.org/10.5194/amt-15-321-2022),
- [2] L. Luo, H. Qin, X. Song, M. Wang H. Qiu, Z. Zhou, *Wireless Sensor Networks for Noise Measurement and Acoustic Event Recognitions in Urban Environments*. *Sensors*. 2020; 20(7): 2093. DOI: [10.3390/s20072093](https://doi.org/10.3390/s20072093).
- [3] L. Maiolo, D. Polese, *Advances in sensing technologies for smart monitoring in precise agriculture*, Proc. of the 10th Int. Conference on Sensor Networks SENSORNETS 2021, Virtual, 9-10 February 2021, 151-158. Online [Accessed 26022023] <https://www.scitepress.org/PublishedPapers/2021/104154/104154.pdf>
- [4] F. Leccese, M. Cagnetti, S. Sciuto, A. Scorza, K. Torokhtii, E. Silva, (2017). Analysis, design, realization and test of a sensor network for aerospace applications, Proc. of the 2017 IEEE Int. Instrumentation and Measurement Technology Conference I2MTC 2017, Turin, Italy, 22-25 May 2017, pp. 1-6. DOI: [10.1109/I2MTC.2017.7969946](https://doi.org/10.1109/I2MTC.2017.7969946)
- [5] P. Hariharan (2007). *Basics of Interferometry*, Second Edition. Elsevier. ISBN 978-0-12-373589-8.
- [6] S. van den Berg, S. van Eldik, N. Bhattacharya, Mode-resolved frequency comb interferometry for high-accuracy long distance measurement. *Sci Rep* 5, 2015, 14661. DOI: [10.1038/srep14661](https://doi.org/10.1038/srep14661)
- [7] EMPIR project 17IND12 MetFoF Metrology for the Factory of the Future, 2018 – 2021. Online [Accessed 21 February 2023] www.met4fof.eu
- [8] G. Kok, Quantifizierung von Redundanz in Sensornetzwerken und die Beziehung zur Messunsicherheit, *tm - Technisches Messen*, 89(10), 2022, pp. 647-657, [In German]. DOI: [10.1515/teme-2022-0012](https://doi.org/10.1515/teme-2022-0012)
- [9] T. Dorst, Influence of synchronization within a sensor network on machine learning results. *J. Sens. Sens. Syst.*, 10, 2021, pp. 233–245. DOI: [10.5194/jsss-10-233-2021](https://doi.org/10.5194/jsss-10-233-2021)
- [10] B. Edlén, The refractive index of air, *Metrologia* vol. 2, no. 2, 1966, pp. 71–80. DOI: [10.1088/0026-1394/2/2/002](https://doi.org/10.1088/0026-1394/2/2/002)
- [11] Zigbee mqtt software. Online [Accessed 21 February 2023] <https://www.zigbee2mqtt.io/guide/getting-started/>
- [12] Zigbee mosquito software. Online [Accessed 21 February 2023] <https://www.mosquitto.org/download/>
- [13] Zigbee sensor node firmware. Online [Accessed 21 February 2023] <https://github.com/ptvoinfo/zigbee-configurable-firmware>
- [14] Zigbee coordinator firmware. Online [Accessed 21 February 2023] https://github.com/Koenkk/Z-Stack-firmware/raw/master/coordinator/Z-Stack_3.x.0/bin/.
- [15] M. Born, E. Wolf, *Principles of Optics*, 1959, New York, NY: Pergamon Press INC.